

Scaleformer: Iterative Multi-scale Refining Transformers for Time Series Forecasting

Mohammad Amin Shabani,
 Simon Fraser University, Canada
 & Borealis AI, Canada
 mshabani@sfu.ca

Amir Abdi, Lili Meng, Tristan Sylvain
 Borealis AI, Canada
 {firstname.lastname}@borealisai.com

Abstract

The performance of time series forecasting has recently been greatly improved by the introduction of transformers. In this paper, we propose a general multi-scale framework that can be applied to state-of-the-art transformer-based time series forecasting models including Autoformer and Informer. Using iteratively refining a forecasted time series at multiple scales with shared weights, architecture adaptations and a specially-designed normalization scheme, we are able to achieve significant performance improvements with minimal additional computational overhead. Via detailed ablation studies, we demonstrate the effectiveness of our proposed architectural and methodological innovations. Furthermore, our experiments on four public datasets show that the proposed multi-scale framework outperforms the corresponding baselines with an average improvement of 13% and 38% over Autoformer and Informer, respectively.

1 Introduction

Integrating information at different time scales is essential to accurately model, and in turn, forecast time series. From weather patterns that fluctuate both locally and globally, as well as throughout the day and across seasons, to radio carrier waves which contain relevant signals at different frequencies, time series forecasting models need to encourage *scale awareness* in learnt representations. While transformer-based architectures have become the mainstream and state-of-the-art for time series forecasting in recent years, advances have focused mainly on mitigating the standard quadratic complexity in time and space, e.g., attention (logSparse [1]) or structural changes (proximity hashing [2]), rather than explicit scale-awareness. The essential cross-scale feature relationships are often learnt implicitly, and are not encouraged by architectural priors of any kind beyond the stacked attention blocks that characterize the transformer models. Autoformer [3] introduced some emphasis on scale-awareness by enforcing different computational paths for the trend and seasonal components of the input time series; however, this structural prior only focused on two scales: low- and high-frequency components. **Given its importance to forecasting, can we make transformers more scale-aware?**

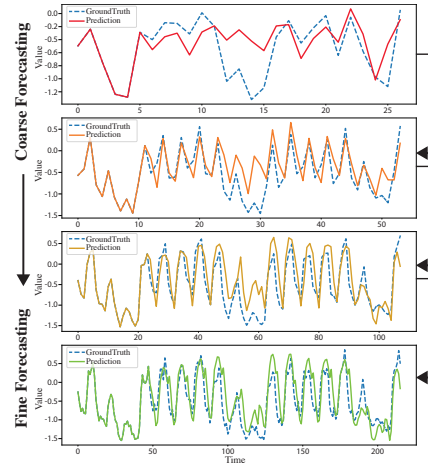


Figure 1: Intermediate forecasts by our model at different time scales. Iterative refinement of a time series forecast is a strong structural prior that benefits time series forecasting.

We enable this with *Scaleformer*. In our proposed approach, showcased in Figure 1, time series forecasts are iteratively refined at successive time-steps, allowing the model to better capture the inter-dependencies and specificities of each scale. However, scale itself is not sufficient. Iterative refinement at different scales can cause significant distribution shifts between intermediate forecasts which can lead to runaway error propagation. To mitigate this issue, we introduce cross-scale normalization at each step.

Our approach re-orders model capacity to shift the focus on scale awareness, but does not fundamentally alter the attention-driven paradigm of transformers. As a result, it can be readily adapted to work jointly with multiple recent time series transformer architectures, acting broadly orthogonally to their own contributions. Leveraging this, we chose to operate with AutoFormer and Informer backbones to further probe the effect of our multi-scale method on a variety of experimental setups.

Our contributions are as follows: (1) we introduce a novel iterative scale-refinement paradigm that can be readily adapted to a variety of transformer-based time series forecasting architectures. (2) To minimize distribution shifts between scales and windows, we introduce cross-scale normalization on outputs of the Transformer. (3) Using Informer and AutoFormer, two state-of-the-art architectures, as backbones, we demonstrate empirically the effectiveness of our approach on a variety of datasets, resulting in an average improvement of 13% over Autoformer and 38% over Informer. (4) Via a detailed ablation study of our findings, we demonstrate the validity of our architectural and methodological choices.

2 Related works

Time-series forecasting: Time-series forecasting plays an important role in many domains, including: weather forecasting [4], inventory planning [5], astronomy [6], economic and financial forecasting [7]. One of the specificities of time series data is the need to capture *seasonal* trends [8]. There exists a vast variety of time-series forecasting models [9, 10, 11, 12, 13, 14]. Early approaches such as ARIMA [9] and exponential smoothing models [10] were followed by the introduction of neural network based approaches involving either Recurrent Neural Networks (RNNs) and their variants [11, 12, 12, 11] or Temporal Convolutional Networks (TCNs) [13].

More recently, time-series Transformers [14, 15] were introduced for the forecasting task by leveraging self-attention mechanisms to learn complex patterns and dynamics from time series data. Binh and Matteson [16] proposes a probabilistic, non-auto-regressive transformer-based model with the integration of state space models. The original quadratic complexity in time and memory was lowered to $O(L \log L)$ by enforcing sparsity in the attention mechanism with the ProbSparse attention of the Informer model [17], and the logSparse attention mechanism [1]. While such attention mechanisms operate on a point-wise basis, Autoformer [3] used a cross-correlation-based attention mechanism to operate at the level of subsequences. This, along with trend/cycle decomposition resulted in improved performance.

Multi-scale neural architectures: Multi-scale and hierarchical processing is useful in many domains, such as computer vision [18, 19, 20], natural language processing [21, 22, 23] and time series forecasting [24, 25]. Multiscale Vision Transformers [18] is proposed for video and image recognition, by connecting the seminal idea of multiscale feature hierarchies with transformer models, however, it focuses on the spatial domain, specially designed for computer vision tasks. Cui et al. [26] proposed to use different transformations of a time series such as downsampling and smoothing in parallel to the original signal to better capture temporal patterns and reduce the effect of random noise. Many different architectures have been proposed recently [27, 28, 29, 30] to improve RNNs in tasks such as language processing, computer vision, time-series analysis, and speech recognition. However, these methods are mainly focused on proposing a new RNN-based module which is not applicable to transformers directly. The same direction has been also investigated in Transformers [22], TCN [31], and MLP [32] models. In the most recent work, Du et al. [33] proposed multi-scale segment-wise correlations as a multi-scale version of the self-attention mechanism. Our work is orthogonal to the above methods as a model-agnostic framework to utilize multi-scale time-series in transformers while keeping the number of parameters and time complexity roughly the same.

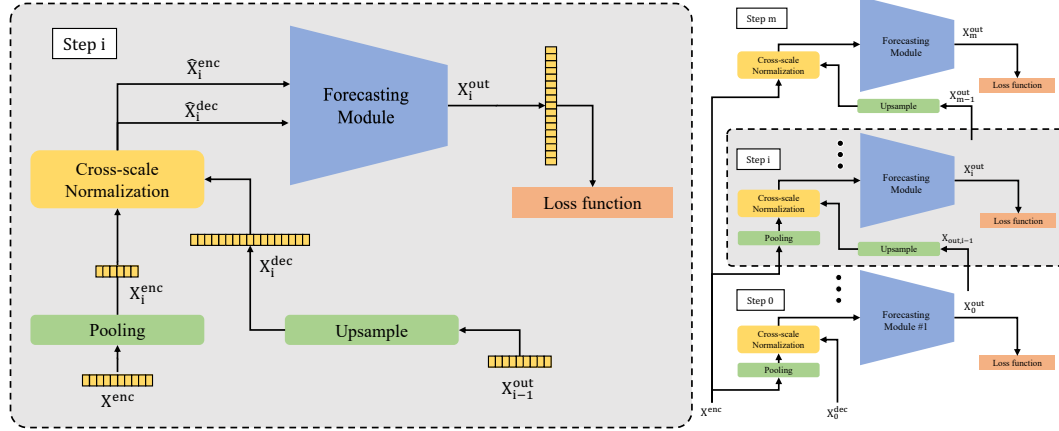


Figure 2: Overview of the proposed framework. (Left) Representation of a single scaling block. In each step, we pass the normalized upsampled version of the output from previous step along with the normalized downsampled version of encoder as the input. (Right) Representation of the full architecture. We process the input in a multi-scale manner iteratively from the smallest scale to the original scale.

3 Problem Setting

We denote $\mathbf{X}^{(L)}$, and $\mathbf{X}^{(H)}$ the look-back and horizon windows for the forecast, respectively, of respective lengths ℓ_L, ℓ_H . Given a starting time t_0 we can express these time-series as follows: $\mathbf{X}^{(L)} = \{\mathbf{x}_t | \mathbf{x}_t \in \mathbb{R}^{d_x}, t \in [t_0, t_0 + \ell_L]\}$ and $\mathbf{X}^{(H)} = \{\mathbf{x}_t | \mathbf{x}_t \in \mathbb{R}^{d_x}, t \in [t_0 + \ell_L + 1, t_0 + \ell_L + \ell_H]\}$. The goal of the forecasting task is to predict the horizon window given the look-back window. Following previous works [3, 17], we pass $\mathbf{X}^{enc} = \mathbf{X}^{(L)}$ as the input to the encoder. While an array of zero-values would be the default to pass to the decoder, the decoder instead takes as input the second half of the look-back window padded with zeros $\mathbf{X}^{dec} = \{\mathbf{x}_{t_0 + \ell_L/2}, \dots, \mathbf{x}_{\ell_L}, 0, 0, \dots, 0\}$ with length $\ell_L/2 + \ell_H$. For the purpose of notational simplicity, we omit references to this half of the look-back window in the equations that follow.

4 Proposed Method

In this section, we first describe the proposed framework in subsection 4.1, and the normalization scheme in subsection 4.2. Then, we provide details on the input's representation in subsection 4.3, and the loss function in subsection 4.4.

4.1 Multi-scale Framework

Our proposed framework applies successive transformer modules to iteratively refine a time-series forecast, at different temporal scales. The proposed framework is shown in Figure 2.

Given an input time-series $\mathbf{X}^{(L)}$, we iteratively apply the same neural module multiple times at different temporal scales. Concretely, we consider a set of scales $S = \{s^m, \dots, s^2, s^1, 1\}$, where $m = \lfloor \log_s \ell_L \rfloor - 1$ and s is a downscaling factor. The input to the encoder at the i -th step ($0 \leq i \leq m$) is the original look-back window $\mathbf{X}^{(L)}$, downsampled by a scale factor of $s_i \equiv s^{m-i}$ via an average pooling operation. The input to the decoder, on the other hand, is \mathbf{X}_{i-1}^{out} upsampled by a factor of s via a linear interpolation. Finally, \mathbf{X}_0^{dec} is initialized to an array of 0s. The model performs the

following operations:

$$\mathbf{x}_{t,i} = \frac{1}{s_i} \sum_{\tau=1}^{\tau+s_i} \mathbf{x}_\tau, \quad \tau = t \times s_i \quad (1)$$

$$\mathbf{X}_i^{(L)} = \left\{ \mathbf{x}_{t,i} \mid \frac{t_0}{s_i} \leq t \leq \frac{t_0 + \ell_L}{s_i} \right\} \quad (2)$$

$$\mathbf{X}_i^{(H)} = \left\{ \mathbf{x}_{t,i} \mid \frac{t_0 + \ell_L + 1}{s_i} \leq t \leq \frac{t_0 + \ell_L + \ell_H}{s_i} \right\}, \quad (3)$$

where $\mathbf{X}_i^{(L)}$ and $\mathbf{X}_i^{(H)}$ are the look-back and horizon windows at the i th step with the scale factor of s^{m-i} and with the lengths of $\ell_{L,i}$ and $\ell_{H,i}$, respectively. Assuming $\mathbf{x}'_{t,i-1}$ is the output of the forecasting module at step $i-1$ and time t , we can define $\mathbf{X}_i^{\text{enc}}$ and $\mathbf{X}_i^{\text{dec}}$ as the inputs to the normalization:

$$\mathbf{X}_i^{\text{enc}} = \mathbf{X}_i^{(L)} \quad (4)$$

$$\mathbf{x}''_{t,i} = \mathbf{x}'_{\lfloor t/s \rfloor, i-1} + (\mathbf{x}'_{\lceil t/s \rceil, i-1} - \mathbf{x}'_{\lfloor t/s \rfloor, i-1}) \times \frac{t - \lfloor t/s \rfloor}{s} \quad (5)$$

$$\mathbf{X}_i^{\text{dec}} = \{ \mathbf{x}''_{t,i} \mid \frac{t_0 + \ell_L + 1}{s_i} \leq t \leq \frac{t_0 + \ell_L + \ell_H}{s_i} \}. \quad (6)$$

Finally, we calculate the error between $\mathbf{X}_i^{(H)}$ and $\mathbf{X}_i^{\text{out}}$ as the loss function to train the model. We discuss the normalization layer in the next section followed by the input embedding in Section 4.3 and the loss function in Section 4.4.

4.2 Cross-scale Normalization

Given a set of input series $(\mathbf{X}_i^{\text{enc}}, \mathbf{X}_i^{\text{dec}})$, with dimensions $\ell_{L,i} \times d_x$ and $\ell_{H,i} \times d_x$, respectively for the encoder and the decoder of the transformer in i th step, we normalize each series based on the temporal average of $\mathbf{X}_i^{\text{enc}}$ and $\mathbf{X}_i^{\text{dec}}$. More formally:

$$\bar{\mu}_{\mathbf{X}_i} = \frac{1}{\ell_{L,i} + \ell_{H,i}} \left(\sum_{\mathbf{x}^{\text{enc}} \in \mathbf{X}_i^{\text{enc}}} \mathbf{x}^{\text{enc}} + \sum_{\mathbf{x}^{\text{dec}} \in \mathbf{X}_i^{\text{dec}}} \mathbf{x}^{\text{dec}} \right) \quad (7)$$

$$\hat{\mathbf{X}}_i^{\text{dec}} = \mathbf{X}_i^{\text{dec}} - \bar{\mu}_{\mathbf{X}_i} \quad (8)$$

$$\hat{\mathbf{X}}_i^{\text{enc}} = \mathbf{X}_i^{\text{enc}} - \bar{\mu}_{\mathbf{X}_i} \quad (9)$$

where $\bar{\mu}_{\mathbf{X}_i} \in \mathbb{R}^{d_x}$ is the average over the temporal dimension of the concatenation of both look-back window and the horizon. Here, $\hat{\mathbf{X}}_i^{\text{enc}}$ and $\hat{\mathbf{X}}_i^{\text{dec}}$ are the inputs of the i th step to the forecasting module.

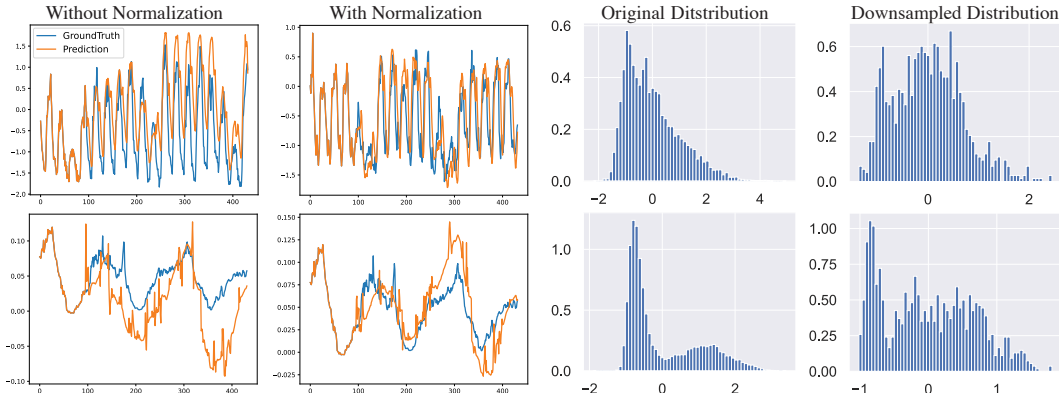


Figure 3: The figure shows the output results of two series using the same trained multi-scale model with and without shifting the data (left) which demonstrates the importance of normalization. On the right, we can see the distribution changes due to the downsampling of two series compared to the original scales from the Electricity dataset.

When the distribution of input to a learning model or its sub-components (e.g., a sub-network or a layer) changes from that of the training data, it experiences a distribution shift [34, 35]. Two distinct types of distribution shifts are common. First, there is a natural distribution shift between the look-back window and the forecast window (the covariate shift). Additionally, there is a distribution shift between the predicted forecast windows at two consecutive scales which is a result of the upsampling operation alongside the error accumulation during the intermediate computations. As a result, normalizing the output at a given step by either the look-back window statistics or the previously predicted forecast window statistics result in an accumulation of errors across steps. We mitigate this by considering a moving average of forecast and look-back statistics as the basis for the output normalization. While this change might appear relatively minor, it has a significant impact on the resulting distributions of outputs as shown in Figure 3. As a result of the improved normalization, it also results in greatly improved performance and is essential to the proposed approach’s performance as shown in Table 2. The improvement is more evident when compared to the alternative approaches, namely, normalizing by either look-back or previous forecast window statistics.

4.3 Input Embedding

Following the previous works, we embed our input to have the same number of features as the hidden dimension of the model. The embedding consists of three parts: (1) *Value embedding* which uses a linear layer to map the input observations of each step \mathbf{x}_t to the same dimension as the model. We further concatenate an additional value 0, 0.5, or 1 respectively showing if each observation is coming from the look-back window, zero initialization, or the prediction of the previous steps. (2) *Temporal Embedding* which again uses a linear layer to embed the time stamp related to each observation to the hidden dimension of the model. Here we concatenate an additional value $1/s_i - 0.5$ as the current scale for the network before passing to the linear layer. (3) We also use a fixed *positional embedding* which is adapted to the different scales s_i as follows:

$$\begin{aligned} PE(pos, 2k, s_i) &= \sin \left(\frac{\text{pos} \times s_i}{10000^{2k/d_{\text{model}}}} \right) \\ PE(pos, 2k + 1, s_i) &= \cos \left(\frac{\text{pos} \times s_i}{10000^{2k/d_{\text{model}}}} \right) \end{aligned} \quad (10)$$

4.4 Loss Function

Using the standard MSE objective to train time-series forecasting models leaves them sensitive to outliers, which are common in some, but not all, of the standard time-series datasets. One possible solution would be to use objectives more robust to outliers, such as the Huber loss [36]. However, when there are no major outliers, such objectives tend to underperform. Given the heterogeneous nature of the datasets we are considering, we instead utilize the adaptive loss first proposed by Barron [37] defined as:

$$f(\xi, \alpha, c) = \frac{|\alpha - 2|}{\alpha} \left(\left(\frac{(\xi/c)^2}{|\alpha - 2|} + 1 \right)^{\alpha/2} - 1 \right) \quad (11)$$

with $\xi = (\mathbf{X}_i^{\text{out}} - \mathbf{X}_i^{(H)})$ in step i . The parameters α and c , which modulate the loss sensitivity to outliers, are learnt in an end-to-end fashion during training. To the best of our knowledge, this is the first time this objective has been adapted to the context of time-series forecasting.

5 Experiments

Baselines: To measure the effectiveness of the proposed framework, we mainly use state-of-the-art models Informer [17] and Autoformer [3] which have already beaten many Transformer-based (e.g. LogTrans [1], Reformer [2]), RNN-based (e.g. LSTMNet [38], LSTM) and TCN [13] models. In order to keep the tables concise and more readable, we omit the these baseline results here. For Informer, we train the model without any changes as the core of our framework. However, Autoformer uses a decomposition layer at the input of the decoder and does not pass the trend series to the network,

which makes the model unaware of the previous predictions. To resolve this, we pass zeros as the trend and the series without decomposition as the input to the decoder.

Implementation Details: Our implementation is based on the Pytorch [39] implementation¹ of the Autoformer and Informer models provided by Xu et al. [3] The hidden dimension of models are fixed to 512 with a batch size of 32, and we train each model for 10 epochs with early stop enabled. To optimize the models, an Adam optimizer has been used with a learning rate of 1e-4 for the forecasting model and 1e-3 for optimizing the adaptive loss. The forecasting module is fixed to 2 encoder layers and 1 decoder layer. The look-back window size is fixed to 96, and the horizon is varied from 96 to 720. We repeat each experiment 5 times to reduce the effect of randomness in the reported values. In all experiments, the temporal scale factor s is fixed to 2 (for more details on the impact of the choice of scaling factor on results, please refer to the appendix). While the loss-modulation parameters α and c could be learnt independently for each series in a given dataset, we found improved performance when considering a single value per dataset.

Datasets: We consider four public datasets with different characteristics to evaluate our proposed framework. **Electricity Consuming Load (ECL)**² corresponds to the electricity consumption (Kwh) of 321 clients. **Traffic**³ aggregates the hourly occupancy rate of 963 car lanes of San Francisco bay area freeways. **Weather**⁴ contains 21 meteorological indicators, such as air temperature, humidity, etc, recorded every 10 minutes for the entirety of 2020. **Exchange-Rate** [38] collects the daily exchange rates of 8 countries (Australia, British, Canada, Switzerland, China, Japan, New Zealand and Singapore) from 1990 to 2016.

5.1 Comparison with the baselines

Table 1 shows the results of the proposed framework and the loss function compared with the baselines. To have a better comparison, each experiment is repeated 5 times, and the average is reported along with the standard deviation. Our proposed multi-scale framework with the adaptive loss function improves the baselines in almost all of the experiments with an average improvement of 13% over Autoformer and 38% over Informer. The improvement is significant, specially in the case of exchange-rate dataset with Informer as the baseline, which achieves more than 50% average improvement over the different horizon lengths.

Time and Memory complexity: The proposed framework uses the same number of parameters for the model as the baselines (except two parameters α and c of the Adaptive loss). Our framework sacrifices a small amount of computation efficiency for the sake of significant performance improvement. Furthermore, we show in the appendix that, if we do not process the final scale, relying instead of a simple interpolation of the prior output, we achieve improved performance over the baselines, at no computational overhead.

5.2 Ablation study

Impact of each sub-component: To verify the performance improvement of both the framework and the adaptive loss function, we trained the models on all four combinations of baselines with and without multi-scale framework and using MSE loss or Adaptive loss functions for training. Table 2 shows the effect of multi-scale and the loss function respectively for Informer and Autoformer.

Comparing the model using the Adaptive loss with the models trained with MSE loss, we can see that in both multi-scale and the original baselines training with adaptive loss improves the performance. The same thing is valid comparing the multi-scale versions versus the original baselines training with either MSE or Adaptive loss functions. The experiments using both the multi-scale framework and Adaptive loss achieve the best results.

Cross-scale normalization: As we discussed in Section 4.2, having the cross-scale normalization is crucial to avoid the distribution shifts. To confirm that, we conduct two experiments. First, by

¹<https://github.com/thuml/Autoformer>

²<https://archive.ics.uci.edu/ml/datasets/ElectricityLoadDiagrams20112014>

³<https://pems.dot.ca.gov>

⁴<https://www.bgc-jena.mpg.de/wetter/>

Table 1: Comparison of the MSE and MAE results for our proposed multi-scale framework version of Informer and Autoformer (-**MSA**) with their original models as the baseline. Results are given in the *multi-variate* setting, for different lengths of the horizon window. The look-back window size is fixed to 96 for all experiments. The best results are shown in **Bold**. Our method outperforms vanilla versions of both Informer and Autoformer over almost all datasets and settings.

Dataset	Autoformer		Autoformer-MSA		Informer		Informer-MSA	
	Metric	MSE	MAE	MSE	MAE	MSE	MAE	MSE
Exchange	96	0.154±0.01	0.285±0.00	0.126 ±0.01	0.259 ±0.01	0.966±0.10	0.792±0.04	0.168 ±0.05
	192	0.356±0.09	0.428±0.05	0.253 ±0.03	0.373 ±0.02	1.088±0.04	0.842±0.01	0.427 ±0.12
	336	0.441 ±0.02	0.495 ±0.01	0.519±0.16	0.538±0.09	1.598±0.08	1.016±0.02	0.500 ±0.05
	720	1.118±0.04	0.819±0.02	0.928 ±0.23	0.751 ±0.09	2.679±0.22	1.340±0.06	1.017 ±0.05
Weather	96	0.267±0.03	0.334±0.02	0.163 ±0.01	0.226 ±0.01	0.388±0.04	0.435±0.03	0.210 ±0.02
	192	0.323±0.01	0.376±0.00	0.221 ±0.01	0.290 ±0.02	0.433±0.05	0.453±0.03	0.289 ±0.01
	336	0.364±0.02	0.397±0.01	0.282 ±0.02	0.340 ±0.03	0.610±0.04	0.551±0.02	0.418 ±0.04
	720	0.425±0.01	0.434±0.01	0.369 ±0.04	0.396 ±0.03	0.978±0.05	0.723±0.02	0.595 ±0.04
Electricity	96	0.197±0.01	0.312±0.01	0.188 ±0.00	0.303 ±0.01	0.344±0.00	0.421±0.00	0.203 ±0.01
	192	0.219±0.01	0.329±0.01	0.197 ±0.00	0.310 ±0.00	0.344±0.01	0.426±0.01	0.219 ±0.00
	336	0.263±0.04	0.359±0.03	0.224 ±0.02	0.333 ±0.01	0.358±0.01	0.440±0.01	0.253 ±0.01
	720	0.290±0.05	0.380±0.02	0.249 ±0.01	0.358 ±0.01	0.386±0.00	0.452±0.00	0.293 ±0.01
Traffic	96	0.628±0.02	0.393±0.02	0.567 ±0.00	0.350 ±0.00	0.748±0.01	0.426±0.01	0.597 ±0.01
	192	0.634±0.01	0.401±0.01	0.589 ±0.01	0.360 ±0.01	0.772±0.02	0.436±0.01	0.655 ±0.01
	336	0.619 ±0.01	0.385±0.01	0.619 ±0.01	0.383 ±0.01	0.868±0.04	0.493±0.03	0.761 ±0.03
	720	0.656±0.01	0.403±0.01	0.642 ±0.01	0.397 ±0.01	1.074±0.02	0.606±0.01	0.924 ±0.02

Table 2: Comparison of training with Adaptive loss "-A", multi-scale framework with MSE loss "-MS", Multi-scale framework and Adaptive loss "-MSA". It shows the combination of all our proposed contributions is essential, and results in significantly improved performance.

Dataset	Informer		Informer-A		Informer-MS		Informer-MSA	
	Metric	MSE	MAE	MSE	MAE	MSE	MAE	MSE
Weather	96	0.388±0.04	0.435±0.03	0.342±0.03	0.382±0.02	0.249±0.02	0.324±0.01	0.210 ±0.02
	192	0.433±0.05	0.453±0.03	0.385±0.02	0.404±0.01	0.315±0.02	0.380±0.02	0.289 ±0.01
	336	0.610±0.04	0.551±0.02	0.656±0.10	0.550±0.04	0.473±0.04	0.478±0.02	0.418 ±0.04
	720	0.978±0.05	0.723±0.02	0.953±0.04	0.680±0.02	0.664±0.04	0.585±0.02	0.595 ±0.04
Electricity	96	0.344±0.00	0.421±0.00	0.321±0.00	0.402±0.00	0.211±0.00	0.326±0.00	0.203 ±0.01
	192	0.344±0.01	0.426±0.01	0.341±0.01	0.422±0.01	0.233±0.01	0.348±0.00	0.219 ±0.00
	336	0.358±0.01	0.440±0.01	0.344±0.00	0.422±0.00	0.279±0.01	0.388±0.01	0.253 ±0.01
	720	0.386±0.00	0.452±0.00	0.363±0.00	0.432±0.00	0.315±0.01	0.411±0.00	0.293 ±0.01

Dataset	Autoformer		Autoformer-A		Autoformer-MS		Autoformer-MSA	
	Metric	MSE	MAE	MSE	MAE	MSE	MAE	MSE
Weather	96	0.267±0.03	0.334±0.02	0.229±0.01	0.288±0.01	0.174±0.01	0.254±0.01	0.163 ±0.01
	192	0.323±0.01	0.376±0.00	0.293±0.02	0.340±0.02	0.250±0.02	0.333±0.02	0.221 ±0.01
	336	0.364±0.02	0.397±0.01	0.357±0.01	0.387±0.01	0.314±0.02	0.380±0.02	0.282 ±0.02
	720	0.425±0.01	0.434±0.01	0.419±0.01	0.422±0.01	0.414±0.03	0.457±0.02	0.369 ±0.04
Electricity	96	0.197±0.01	0.312±0.01	0.201±0.01	0.312±0.01	0.196±0.00	0.312±0.01	0.188 ±0.00
	192	0.219±0.01	0.329±0.01	0.221±0.01	0.328±0.01	0.208±0.00	0.323±0.00	0.197 ±0.00
	336	0.263±0.04	0.359±0.03	0.232±0.01	0.339±0.01	0.220 ±0.00	0.336±0.00	0.224±0.02
	720	0.290±0.05	0.380±0.02	0.249 ±0.01	0.351 ±0.01	0.252±0.00	0.364±0.00	0.249±0.01

using the multi-scale framework without having the cross-scale normalization, we argue that the error accumulation and covariate shift between the scales will lead to a higher error than using only a single scale. As it is shown in Table 3, while the multi-scale framework can get better results in few cases, it mostly have higher errors that baselines.

On the other hand, adding the normalization while having a single scale can still help to achieve better performance by reducing the effect of covariate shift between the training and the test series. As we can see in table 4, the normalization will improve the results of Informer consistently while for the Autoformer, the original decomposition layer for the input already solve that problem and replacing that with our normalization can only reduce the capacity of the model.

Table 3: Multi-scale framework without cross-scale normalization. Correctly normalizing across different scales (as per our cross-mean normalization) is essential to obtain good performance when using a multi-scale framework such as ours

Dataset	Autoformer		Autoformer-MS (w/o N)		Informer		Informer-MS (w/o N)	
	Metric	MSE	MAE	MSE	MAE	MSE	MAE	MSE
Weather	96	0.267±0.03	0.334±0.02	0.191±0.02	0.277±0.02	0.388±0.04	0.435±0.03	0.402±0.05
	192	0.323±0.01	0.376±0.00	0.281±0.04	0.360±0.03	0.433±0.05	0.453±0.03	0.393±0.04
	336	0.364±0.02	0.397±0.01	0.376±0.08	0.420±0.04	0.610±0.04	0.551±0.02	0.566±0.04
	720	0.425±0.01	0.434±0.01	0.439±0.04	0.465±0.02	0.978±0.05	0.723±0.02	1.293±0.10
Electricity	96	0.197±0.01	0.312±0.01	0.221±0.01	0.337±0.01	0.344±0.00	0.421±0.00	0.407±0.02
	192	0.219±0.01	0.329±0.01	0.251±0.00	0.357±0.00	0.344±0.01	0.426±0.01	0.407±0.02
	336	0.263±0.04	0.359±0.03	0.288±0.01	0.380±0.01	0.358±0.01	0.440±0.01	0.392±0.02
	720	0.290±0.05	0.380±0.02	0.309±0.00	0.397±0.00	0.386±0.00	0.452±0.00	0.391±0.01

Table 4: Single-scale framework with cross scale normalization "-N". The cross-scale normalization (which in the single-scale case corresponds to mean-normalization of the output) does not improve the performance of the Autoformer, as it already has an internal trend-cycle normalization component. However, it does improve the results of the Informer.

Dataset	Autoformer		Autoformer-N		Informer		Informer-N	
	Metric	MSE	MAE	MSE	MAE	MSE	MAE	MSE
Weather	96	0.267±0.03	0.334±0.02	0.323±0.01	0.401±0.01	0.388±0.04	0.435±0.03	0.253±0.03
	192	0.323±0.01	0.376±0.00	0.531±0.04	0.543±0.02	0.433±0.05	0.453±0.03	0.357±0.02
	336	0.364±0.02	0.397±0.01	0.859±0.06	0.708±0.03	0.610±0.04	0.551±0.02	0.459±0.03
	720	0.425±0.01	0.434±0.01	1.682±0.08	1.028±0.02	0.978±0.05	0.723±0.02	0.870±0.03
Electricity	96	0.197±0.01	0.312±0.01	0.251±0.01	0.364±0.01	0.344±0.00	0.421±0.00	0.247±0.00
	192	0.219±0.01	0.329±0.01	0.263±0.00	0.372±0.00	0.344±0.01	0.426±0.01	0.291±0.01
	336	0.263±0.04	0.359±0.03	0.276±0.01	0.388±0.01	0.358±0.01	0.440±0.01	0.321±0.01
	720	0.290±0.05	0.380±0.02	0.280±0.01	0.385±0.01	0.386±0.00	0.452±0.00	0.362±0.00

5.3 Qualitative Results

Figure 4 shows the prediction of our model $\mathbf{X}_i^{\text{out}}$ for the horizon $\mathbf{X}_i^{(H)}$ concatenated with the given look-back window $\mathbf{X}_i^{(L)}$ for two different series and scales $\{16, 8, 4, 2\}$. It shows that the model is able to improve its initial forecast on the smaller scales.

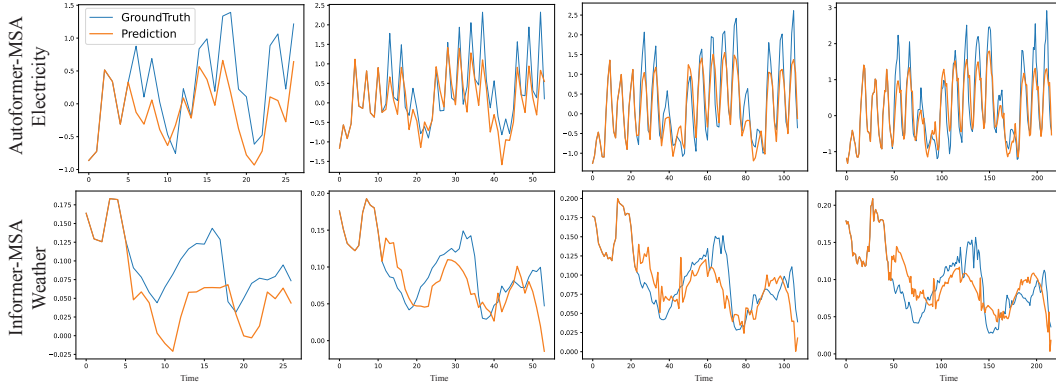


Figure 4: Qualitative results of each scale. The model can correct its previous mistakes on higher scales, showcasing increased robustness to forecasting artifacts that occur individually at each scale.

We have also shown the qualitative comparisons between the vanilla Autoformer and Informer versus the results of our framework in Figure 5. Most notably, in both cases our approach appears significantly better at forecasting the statistical properties (such as local variance) of the signal.

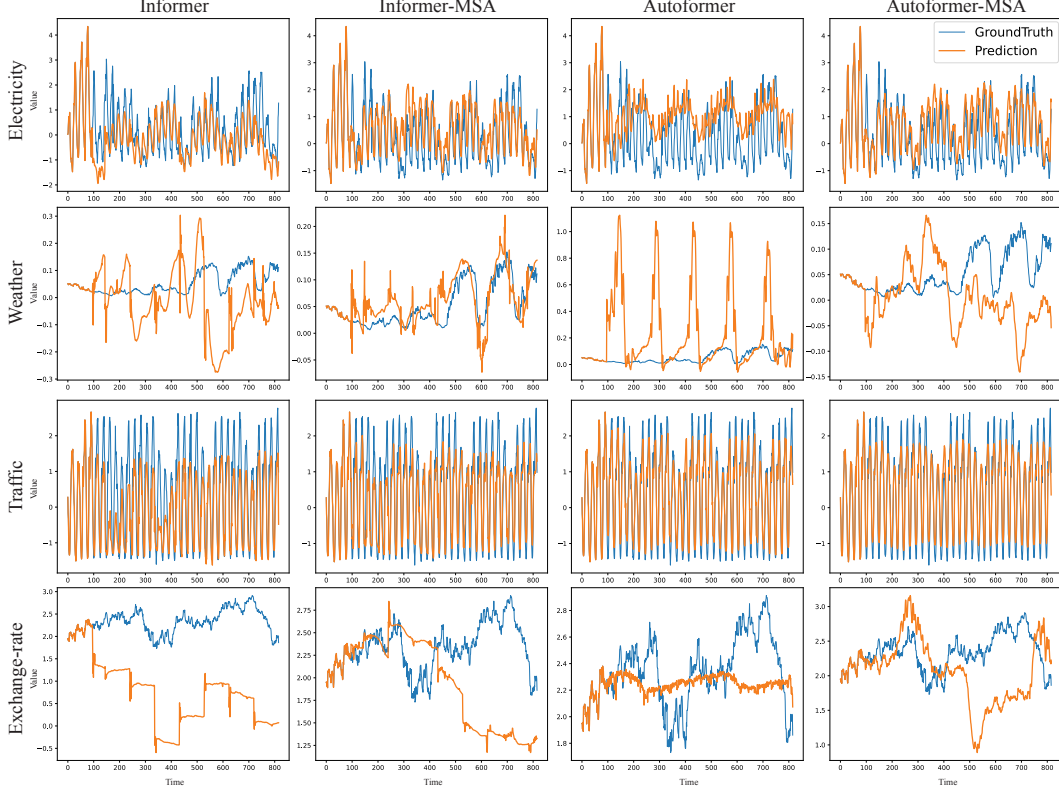


Figure 5: Qualitative comparison of the baselines with our framework version. As we can see, our approach results in qualitatively, as well as quantitatively improved time-series forecasts. The multi-scale transformers are better than their single-scale equivalents at accurately capturing the trend and local variations of the signal.

6 Conclusion

Noting that introducing structural priors that account for multi-scale information is essential for accurate time-series forecastings, this paper proposes a new multi-scale framework on top of recent state-the-art methods for time-series forecasting using Transformers. Our framework iteratively refines a forecasted time-series at increasingly fine-grained scales, and introduces a normalization scheme that minimizes distribution shifts between scales. These contributions result in vastly improved performance over baseline transformer architectures, and qualitatively result in forecasts that better capture the trend and local variations of the target signal. Additionally, our detailed ablation study shows that the different components synergistically work together to deliver this outcome.

References

- [1] Shiyang Li, Xiaoyong Jin, Yao Xuan, Xiyou Zhou, Wenhui Chen, Yu-Xiang Wang, and Xifeng Yan. Enhancing the locality and breaking the memory bottleneck of transformer on time series forecasting. *Advances in Neural Information Processing Systems*, 32:5243–5253, 2019.
- [2] Nikita Kitaev, Lukasz Kaiser, and Anselm Levskaya. Reformer: The efficient transformer. In *International Conference on Learning Representations*, 2020.
- [3] Jiehui Xu, Jianmin Wang, Mingsheng Long, et al. Autoformer: Decomposition transformers with auto-correlation for long-term series forecasting. *Advances in Neural Information Processing Systems*, 34, 2021.
- [4] Allan H Murphy. What is a good forecast? an essay on the nature of goodness in weather forecasting. *Weather and forecasting*, 8(2):281–293, 1993.

- [5] Aris A Syntetos, John E Boylan, and Stephen M Disney. Forecasting for inventory planning: a 50-year review. *Journal of the Operational Research Society*, 60(1):S149–S160, 2009.
- [6] Jeffery D Scargle. Studies in astronomical time series analysis. i-modeling random processes in the time domain. *The Astrophysical Journal Supplement Series*, 45:1–71, 1981.
- [7] Bjoern Krollner, Bruce J Vanstone, Gavin R Finnie, et al. Financial time series forecasting with machine learning techniques: a survey. In *ESANN*, 2010.
- [8] Peter J Brockwell and Richard A Davis. *Time series: theory and methods*. Springer Science & Business Media, 2009.
- [9] George EP Box and Gwilym M Jenkins. Some recent advances in forecasting and control. *Journal of the Royal Statistical Society. Series C (Applied Statistics)*, 17(2):91–109, 1968.
- [10] Rob Hyndman, Anne B Koehler, J Keith Ord, and Ralph D Snyder. *Forecasting with exponential smoothing: the state space approach*. Springer Science & Business Media, 2008.
- [11] David Salinas, Valentin Flunkert, Jan Gasthaus, and Tim Januschowski. Deepar: Probabilistic forecasting with autoregressive recurrent networks. *International Journal of Forecasting*, 36(3):1181–1191, 2020.
- [12] Syama Sundar Rangapuram, Matthias W Seeger, Jan Gasthaus, Lorenzo Stella, Yuyang Wang, and Tim Januschowski. Deep state space models for time series forecasting. *Advances in neural information processing systems*, 31, 2018.
- [13] Shaojie Bai, J. Zico Kolter, and Vladlen Koltun. An empirical evaluation of generic convolutional and recurrent networks for sequence modeling. *arXiv:1803.01271*, 2018.
- [14] Neo Wu, Bradley Green, Xue Ben, and Shawn O’Banion. Deep transformer models for time series forecasting: The influenza prevalence case. *arXiv preprint arXiv:2001.08317*, 2020.
- [15] George Zerveas, Srideepika Jayaraman, Dhaval Patel, Anuradha Bhamidipaty, and Carsten Eickhoff. A transformer-based framework for multivariate time series representation learning. In *Proceedings of the 27th ACM SIGKDD Conference on Knowledge Discovery & Data Mining*, pages 2114–2124, 2021.
- [16] Binh Tang and David S Matteson. Probabilistic transformer for time series analysis. *Advances in Neural Information Processing Systems*, 34:23592–23608, 2021.
- [17] Haoyi Zhou, Shanghang Zhang, Jieqi Peng, Shuai Zhang, Jianxin Li, Hui Xiong, and Wancai Zhang. Informer: Beyond efficient transformer for long sequence time-series forecasting. In *Proceedings of AAAI*, 2021.
- [18] Haoqi Fan, Bo Xiong, Karttikeya Mangalam, Yanghao Li, Zhicheng Yan, Jitendra Malik, and Christoph Feichtenhofer. Multiscale vision transformers. In *Proceedings of the IEEE/CVF International Conference on Computer Vision*, pages 6824–6835, 2021.
- [19] Pengchuan Zhang, Xiyang Dai, Jianwei Yang, Bin Xiao, Lu Yuan, Lei Zhang, and Jianfeng Gao. Multi-scale vision longformer: A new vision transformer for high-resolution image encoding. In *Proceedings of the IEEE/CVF International Conference on Computer Vision*, pages 2998–3008, 2021.
- [20] Pengju Liu, Hongzhi Zhang, Kai Zhang, Liang Lin, and Wangmeng Zuo. Multi-level wavelet-cnn for image restoration. In *Proceedings of the IEEE conference on computer vision and pattern recognition workshops*, pages 773–782, 2018.
- [21] Piotr Nawrot, Szymon Tworkowski, Michał Tyrolski, Łukasz Kaiser, Yuhuai Wu, Christian Szegedy, and Henryk Michalewski. Hierarchical transformers are more efficient language models. *arXiv preprint arXiv:2110.13711*, 2021.
- [22] Sandeep Subramanian, Ronan Collobert, Marc’Aurelio Ranzato, and Y-Lan Boureau. Multi-scale transformer language models. *arXiv preprint arXiv:2005.00581*, 2020.
- [23] Yucheng Zhao, Chong Luo, Zheng-Jun Zha, and Wenjun Zeng. Multi-scale group transformer for long sequence modeling in speech separation. In *Proceedings of the Twenty-Ninth International Conference on International Joint Conferences on Artificial Intelligence*, pages 3251–3257, 2021.
- [24] Ling Chen, Donghui Chen, Zongjiang Shang, Youdong Zhang, Bo Wen, and Chenghu Yang. Multi-scale adaptive graph neural network for multivariate time series forecasting. *arXiv preprint arXiv:2201.04828*, 2022.

[25] Qianggang Ding, Sifan Wu, Hao Sun, Jiadong Guo, and Jian Guo. Hierarchical multi-scale gaussian transformer for stock movement prediction. In *IJCAI*, pages 4640–4646, 2020.

[26] Zhicheng Cui, Wenlin Chen, and Yixin Chen. Multi-scale convolutional neural networks for time series classification. *arXiv preprint arXiv:1603.06995*, 2016.

[27] Junyoung Chung, Sungjin Ahn, and Yoshua Bengio. Hierarchical multiscale recurrent neural networks. *arXiv preprint arXiv:1609.01704*, 2016.

[28] Zhengping Che, Sanjay Purushotham, Guangyu Li, Bo Jiang, and Yan Liu. Hierarchical deep generative models for multi-rate multivariate time series. In *International Conference on Machine Learning*, pages 784–793. PMLR, 2018.

[29] Lifeng Shen, Zuocong Li, and James Kwok. Timeseries anomaly detection using temporal hierarchical one-class network. *Advances in Neural Information Processing Systems*, 33:13016–13026, 2020.

[30] Zipeng Chen, Qianli Ma, and Zhenxi Lin. Time-aware multi-scale rnns for time series modeling. In *IJCAI*, 2021.

[31] Minhao Liu, Ailing Zeng, Zhijian Xu, Qixia Lai, and Qiang Xu. Time series is a special sequence: Forecasting with sample convolution and interaction. *arXiv preprint arXiv:2106.09305*, 2021.

[32] Cristian Challu, Kin G Olivares, Boris N Oreshkin, Federico Garza, Max Mergenthaler, and Artur Dubrawski. N-hits: Neural hierarchical interpolation for time series forecasting. *arXiv preprint arXiv:2201.12886*, 2022.

[33] Dazhao Du, Bing Su, and Zhewei Wei. Preformer: Predictive transformer with multi-scale segment-wise correlations for long-term time series forecasting. *arXiv preprint arXiv:2202.11356*, 2022.

[34] Hidetoshi Shimodaira. Improving predictive inference under covariate shift by weighting the log-likelihood function. *Journal of statistical planning and inference*, 90(2):227–244, 2000.

[35] Sergey Ioffe and Christian Szegedy. Batch normalization: Accelerating deep network training by reducing internal covariate shift. In *International conference on machine learning*, pages 448–456. PMLR, 2015.

[36] Peter J. Huber. Robust Estimation of a Location Parameter. *The Annals of Mathematical Statistics*, 35(1):73 – 101, 1964.

[37] Jonathan T Barron. A general and adaptive robust loss function. In *Proceedings of the IEEE/CVF Conference on Computer Vision and Pattern Recognition*, pages 4331–4339, 2019.

[38] Guokun Lai, Wei-Cheng Chang, Yiming Yang, and Hanxiao Liu. Modeling long-and short-term temporal patterns with deep neural networks. In *The 41st International ACM SIGIR Conference on Research & Development in Information Retrieval*, pages 95–104, 2018.

[39] Adam Paszke, Sam Gross, Francisco Massa, Adam Lerer, James Bradbury, Gregory Chanan, Trevor Killeen, Zeming Lin, Natalia Gimelshein, Luca Antiga, Alban Desmaison, Andreas Kopf, Edward Yang, Zachary DeVito, Martin Raison, Alykhan Tejani, Sasank Chilamkurthy, Benoit Steiner, Lu Fang, Junjie Bai, and Soumith Chintala. Pytorch: An imperative style, high-performance deep learning library. In H. Wallach, H. Larochelle, A. Beygelzimer, F. d’Alché-Buc, E. Fox, and R. Garnett, editors, *Advances in Neural Information Processing Systems 32*, pages 8024–8035. Curran Associates, Inc., 2019.

Appendices

A Reducing computational cost

Table 5 shows the impact of replacing the Scaleformer operation at the real scale by an interpolation of values of the previous scale, i.e., at scale s^0 we do not apply the transformer but rather compute the results by linear interpolation of $\mathbf{X}_{m-1}^{\text{out}}$, thereby reducing the compute cost. This lower cost alternative results in better performance than the baselines, yet worse results than the full Scaleformer. This shows that adding scale is indeed more efficient, and that there is the possibility of a trade-off between further improved performance (full Scaleformer) or improved computational efficiency (interpolated Scaleformer).

Table 5: Comparison of the MSE and MAE results for our proposed multi-scale framework version of Informer and Autoformer by removing the last step and using an interpolation instead ($-\mathbf{MSA}_r$) with the corresponding original models as the baseline. Results are given in the *multi-variate* setting, for different lengths of the horizon window. The look-back window size is fixed to 96 for all experiments. The best results are shown in **Bold**. Our method outperforms vanilla versions of both Informer and Autoformer over almost all datasets and settings.

Dataset	Metric	Autoformer		Autoformer- \mathbf{MSA}_r		Informer		Informer- \mathbf{MSA}_r	
		MSE	MAE	MSE	MAE	MSE	MAE	MSE	MAE
Exchange	96	0.154 \pm 0.01	0.285 \pm 0.00	0.132 \pm 0.02	0.265 \pm 0.02	0.966 \pm 0.10	0.792 \pm 0.04	0.248 \pm 0.07	0.366 \pm 0.06
	192	0.356 \pm 0.09	0.428 \pm 0.05	0.418 \pm 0.22	0.466 \pm 0.12	1.088 \pm 0.04	0.842 \pm 0.01	0.727 \pm 0.19	0.637 \pm 0.09
	336	0.441 \pm 0.02	0.495 \pm 0.01	0.736 \pm 0.25	0.629 \pm 0.10	1.598 \pm 0.08	1.016 \pm 0.02	0.643 \pm 0.03	0.620 \pm 0.02
	720	1.118 \pm 0.04	0.819 \pm 0.02	0.773 \pm 0.26	0.709 \pm 0.13	2.679 \pm 0.22	1.340 \pm 0.06	1.036 \pm 0.08	0.803 \pm 0.03
Weather	96	0.267 \pm 0.03	0.334 \pm 0.02	0.168 \pm 0.01	0.239 \pm 0.02	0.388 \pm 0.04	0.435 \pm 0.03	0.211 \pm 0.01	0.278 \pm 0.01
	192	0.323 \pm 0.01	0.376 \pm 0.00	0.226 \pm 0.01	0.296 \pm 0.01	0.433 \pm 0.05	0.453 \pm 0.03	0.288 \pm 0.03	0.336 \pm 0.02
	336	0.364 \pm 0.02	0.397 \pm 0.01	0.298 \pm 0.02	0.351 \pm 0.02	0.610 \pm 0.04	0.551 \pm 0.02	0.459 \pm 0.02	0.445 \pm 0.02
	720	0.425 \pm 0.01	0.434 \pm 0.01	0.412 \pm 0.04	0.434 \pm 0.03	0.978 \pm 0.05	0.723 \pm 0.02	0.593 \pm 0.07	0.528 \pm 0.04
Electricity	96	0.197 \pm 0.01	0.312 \pm 0.01	0.189 \pm 0.00	0.305 \pm 0.00	0.344 \pm 0.00	0.421 \pm 0.00	0.194 \pm 0.00	0.308 \pm 0.00
	192	0.219 \pm 0.01	0.329 \pm 0.01	0.207 \pm 0.00	0.323 \pm 0.00	0.344 \pm 0.01	0.426 \pm 0.01	0.212 \pm 0.00	0.327 \pm 0.00
	336	0.263 \pm 0.04	0.359 \pm 0.03	0.225 \pm 0.01	0.339 \pm 0.00	0.358 \pm 0.01	0.440 \pm 0.01	0.246 \pm 0.00	0.357 \pm 0.00
	720	0.290 \pm 0.05	0.380 \pm 0.02	0.250 \pm 0.01	0.361 \pm 0.01	0.386 \pm 0.00	0.452 \pm 0.00	0.283 \pm 0.01	0.386 \pm 0.01
Traffic	96	0.628 \pm 0.02	0.393 \pm 0.02	0.585 \pm 0.01	0.365 \pm 0.01	0.748 \pm 0.01	0.426 \pm 0.01	0.595 \pm 0.00	0.362 \pm 0.00
	192	0.634 \pm 0.01	0.401 \pm 0.01	0.606 \pm 0.01	0.375 \pm 0.01	0.772 \pm 0.02	0.436 \pm 0.01	0.629 \pm 0.00	0.381 \pm 0.00
	336	0.619 \pm 0.01	0.385 \pm 0.01	0.631 \pm 0.02	0.400 \pm 0.01	0.868 \pm 0.04	0.493 \pm 0.03	0.692 \pm 0.01	0.410 \pm 0.01
	720	0.656 \pm 0.01	0.403 \pm 0.01	0.660 \pm 0.00	0.418 \pm 0.01	1.074 \pm 0.02	0.606 \pm 0.01	0.803 \pm 0.01	0.461 \pm 0.00

B Full ablation studies

Table 6 extends the results of Table 2 of the paper to all four datasets, in the multivariate setting and for the two backbones, Autoformer and Informer.

Table 6: Comparison of training with either only an Adaptive loss "-A", only the multi-scale framework with MSE loss "-MS", or the whole Multi-scale framework and Adaptive loss "-MSA". The results confirm that the combination of all our proposed contributions is essential, and results in significantly improved performance in both Informer and Autoformer. Experiments are done in the multi-variate setting.

Dataset	Informer		Informer-A		Informer-MS		Informer-MSA	
	Metric	MSE	MAE	MSE	MAE	MSE	MAE	MSE
Exchange	96	0.966±0.10	0.792±0.04	0.962±0.09	0.796±0.04	0.201±0.05	0.325±0.03	0.168 ±0.05
	192	1.088±0.04	0.842±0.01	1.106±0.03	0.853±0.01	0.446±0.14	0.502±0.07	0.427 ±0.12
	336	1.598±0.08	1.016±0.02	1.602±0.07	1.019±0.01	0.520±0.05	0.540±0.02	0.500 ±0.05
	720	2.679±0.22	1.340±0.06	2.719±0.19	1.351±0.06	0.997 ±0.08	0.783 ±0.02	1.017±0.05
Weather	96	0.388±0.04	0.435±0.03	0.342±0.03	0.382±0.02	0.249±0.02	0.324±0.01	0.210 ±0.02
	192	0.433±0.05	0.453±0.03	0.385±0.02	0.404±0.01	0.315±0.02	0.380±0.02	0.289 ±0.01
	336	0.610±0.04	0.551±0.02	0.656±0.10	0.550±0.04	0.473±0.04	0.478±0.02	0.418 ±0.04
	720	0.978±0.05	0.723±0.02	0.953±0.04	0.680±0.02	0.664±0.04	0.585±0.02	0.595 ±0.04
Electricity	96	0.344±0.00	0.421±0.00	0.321±0.00	0.402±0.00	0.211±0.00	0.326±0.00	0.203 ±0.01
	192	0.344±0.01	0.426±0.01	0.341±0.01	0.422±0.01	0.233±0.01	0.348±0.00	0.219 ±0.00
	336	0.358±0.01	0.440±0.01	0.344±0.00	0.422±0.00	0.279±0.01	0.388±0.01	0.253 ±0.01
	720	0.386±0.00	0.452±0.00	0.363±0.00	0.432±0.00	0.315±0.01	0.411±0.00	0.293 ±0.01
Traffic	96	0.748±0.01	0.426±0.01	0.744±0.02	0.413±0.01	0.602±0.01	0.375±0.01	0.597 ±0.01
	192	0.772±0.02	0.436±0.01	0.765±0.01	0.416±0.01	0.669±0.01	0.412±0.00	0.655 ±0.01
	336	0.868±0.04	0.493±0.03	0.852±0.05	0.461±0.03	0.815±0.03	0.501±0.02	0.761 ±0.03
	720	1.074±0.02	0.606±0.01	1.030±0.05	0.539±0.03	0.949±0.01	0.556±0.02	0.924 ±0.02

Dataset	Autoformer		Autoformer-A		Autoformer-MS		Autoformer-MSA	
	Metric	MSE	MAE	MSE	MAE	MSE	MAE	MSE
Exchange	96	0.154±0.01	0.285±0.00	0.152±0.01	0.282±0.00	0.145±0.02	0.276±0.01	0.126 ±0.01
	192	0.356±0.09	0.428±0.05	0.342±0.10	0.421±0.06	0.247 ±0.02	0.366 ±0.01	0.253±0.03
	336	0.441 ±0.02	0.495 ±0.01	0.566±0.22	0.554±0.10	0.456±0.08	0.514±0.05	0.519±0.16
	720	1.118±0.04	0.819±0.02	1.120±0.24	0.811±0.10	0.729 ±0.16	0.679 ±0.08	0.928±0.23
Weather	96	0.267±0.03	0.334±0.02	0.229±0.01	0.288±0.01	0.174±0.01	0.254±0.01	0.163 ±0.01
	192	0.323±0.01	0.376±0.00	0.293±0.02	0.340±0.02	0.250±0.02	0.333±0.02	0.221 ±0.01
	336	0.364±0.02	0.397±0.01	0.357±0.01	0.387±0.01	0.314±0.02	0.380±0.02	0.282 ±0.02
	720	0.425±0.01	0.434±0.01	0.419±0.01	0.422±0.01	0.414±0.03	0.457±0.02	0.369 ±0.04
Electricity	96	0.197±0.01	0.312±0.01	0.201±0.01	0.312±0.01	0.196±0.00	0.312±0.01	0.188 ±0.00
	192	0.219±0.01	0.329±0.01	0.221±0.01	0.328±0.01	0.208±0.00	0.323±0.00	0.197 ±0.00
	336	0.263±0.04	0.359±0.03	0.232±0.01	0.339±0.01	0.220 ±0.00	0.336±0.00	0.224±0.02
	720	0.290±0.05	0.380±0.02	0.249 ±0.01	0.351 ±0.01	0.252±0.00	0.364±0.00	0.249±0.01
Traffic	96	0.628±0.02	0.393±0.02	0.610±0.02	0.381±0.01	0.580±0.01	0.358±0.00	0.567 ±0.00
	192	0.634±0.01	0.401±0.01	0.633±0.02	0.396±0.02	0.601±0.00	0.369±0.00	0.589 ±0.01
	336	0.619±0.01	0.385±0.01	0.618 ±0.00	0.381 ±0.00	0.639±0.02	0.397±0.01	0.619±0.01
	720	0.656±0.01	0.403±0.01	0.654±0.02	0.397 ±0.01	0.680±0.02	0.427±0.01	0.642 ±0.01

C Results on different scales

Table 7 showcases the results of our model using different values of the scale parameter s . It shows that a scale of 2 results in better performance.

Table 7: Comparison of the baselines with our method using different scales. Reducing the scale factor from $s = 16$ to $s = 2$ increases the number of steps but achieves lower error on average.

Dataset		Informer		Informer-MSA(s=16)		Informer-MSA(s=4)		Informer-MSA(s=2)	
Metric		MSE	MAE	MSE	MAE	MSE	MAE	MSE	MAE
Exchange	96	0.966 \pm 0.10	0.792 \pm 0.04	0.376 \pm 0.08	0.480 \pm 0.04	0.246 \pm 0.06	0.374 \pm 0.04	0.168 \pm 0.05	0.298 \pm 0.03
	192	1.088 \pm 0.04	0.842 \pm 0.01	0.878 \pm 0.08	0.721 \pm 0.03	0.661 \pm 0.20	0.617 \pm 0.09	0.427 \pm 0.12	0.484 \pm 0.06
	336	1.598 \pm 0.08	1.016 \pm 0.02	0.899 \pm 0.07	0.733 \pm 0.03	0.697 \pm 0.10	0.648 \pm 0.05	0.500 \pm 0.05	0.535 \pm 0.02
	720	2.679 \pm 0.22	1.340 \pm 0.06	1.633 \pm 0.14	1.031 \pm 0.05	1.457 \pm 0.27	0.958 \pm 0.09	1.017 \pm 0.05	0.790 \pm 0.02
Weather	96	0.388 \pm 0.04	0.435 \pm 0.03	0.208 \pm 0.02	0.275 \pm 0.02	0.189 \pm 0.01	0.259 \pm 0.01	0.210 \pm 0.02	0.279 \pm 0.02
	192	0.433 \pm 0.05	0.453 \pm 0.03	0.302 \pm 0.02	0.354 \pm 0.02	0.287 \pm 0.02	0.333 \pm 0.01	0.289 \pm 0.01	0.333 \pm 0.01
	336	0.610 \pm 0.04	0.551 \pm 0.02	0.470 \pm 0.06	0.456 \pm 0.04	0.420 \pm 0.03	0.433 \pm 0.02	0.418 \pm 0.04	0.427 \pm 0.03
	720	0.978 \pm 0.05	0.723 \pm 0.02	0.639 \pm 0.07	0.544 \pm 0.04	0.627 \pm 0.07	0.543 \pm 0.04	0.595 \pm 0.04	0.532 \pm 0.02
Electricity	96	0.344 \pm 0.00	0.421 \pm 0.00	0.215 \pm 0.00	0.329 \pm 0.00	0.203 \pm 0.00	0.315 \pm 0.00	0.203 \pm 0.01	0.315 \pm 0.01
	192	0.344 \pm 0.01	0.426 \pm 0.01	0.257 \pm 0.01	0.370 \pm 0.01	0.235 \pm 0.01	0.347 \pm 0.01	0.219 \pm 0.00	0.331 \pm 0.00
	336	0.358 \pm 0.01	0.440 \pm 0.01	0.300 \pm 0.04	0.400 \pm 0.03	0.264 \pm 0.01	0.373 \pm 0.01	0.253 \pm 0.01	0.360 \pm 0.01
	720	0.386 \pm 0.00	0.452 \pm 0.00	0.334 \pm 0.03	0.418 \pm 0.02	0.306 \pm 0.01	0.401 \pm 0.01	0.293 \pm 0.01	0.390 \pm 0.01
Traffic	96	0.748 \pm 0.01	0.426 \pm 0.01	0.648 \pm 0.02	0.386 \pm 0.01	0.616 \pm 0.00	0.374 \pm 0.01	0.597 \pm 0.01	0.369 \pm 0.00
	192	0.772 \pm 0.02	0.436 \pm 0.01	0.679 \pm 0.01	0.391 \pm 0.01	0.686 \pm 0.01	0.404 \pm 0.01	0.655 \pm 0.01	0.399 \pm 0.01
	336	0.868 \pm 0.04	0.493 \pm 0.03	0.811 \pm 0.02	0.455 \pm 0.01	0.782 \pm 0.03	0.451 \pm 0.02	0.761 \pm 0.03	0.455 \pm 0.03
	720	1.074 \pm 0.02	0.606 \pm 0.01	1.020 \pm 0.07	0.542 \pm 0.03	0.965 \pm 0.03	0.521 \pm 0.01	0.924 \pm 0.02	0.521 \pm 0.01
Dataset		Autoformer		Autoformer-MSA(16)		Autoformer-MSA(4)		Autoformer-MSA(2)	
Metric		MSE	MAE	MSE	MAE	MSE	MAE	MSE	MAE
Exchange	96	0.154 \pm 0.01	0.285 \pm 0.00	0.182 \pm 0.03	0.316 \pm 0.03	0.170 \pm 0.03	0.304 \pm 0.02	0.126 \pm 0.01	0.259 \pm 0.01
	192	0.356 \pm 0.09	0.428 \pm 0.05	0.514 \pm 0.18	0.557 \pm 0.10	0.359 \pm 0.14	0.443 \pm 0.08	0.253 \pm 0.03	0.373 \pm 0.02
	336	0.441 \pm 0.02	0.495 \pm 0.01	0.527 \pm 0.07	0.570 \pm 0.04	0.606 \pm 0.18	0.585 \pm 0.10	0.519 \pm 0.16	0.538 \pm 0.09
	720	1.118 \pm 0.04	0.819 \pm 0.02	1.019 \pm 0.18	0.819 \pm 0.08	0.973 \pm 0.22	0.809 \pm 0.09	0.928 \pm 0.23	0.751 \pm 0.09
Weather	96	0.267 \pm 0.03	0.334 \pm 0.02	0.169 \pm 0.00	0.239 \pm 0.01	0.164 \pm 0.00	0.234 \pm 0.01	0.163 \pm 0.01	0.226 \pm 0.01
	192	0.323 \pm 0.01	0.376 \pm 0.00	0.240 \pm 0.03	0.310 \pm 0.03	0.229 \pm 0.01	0.299 \pm 0.02	0.221 \pm 0.01	0.290 \pm 0.02
	336	0.364 \pm 0.02	0.397 \pm 0.01	0.304 \pm 0.03	0.354 \pm 0.03	0.303 \pm 0.01	0.350 \pm 0.01	0.282 \pm 0.02	0.340 \pm 0.03
	720	0.425 \pm 0.01	0.434 \pm 0.01	0.375 \pm 0.01	0.403 \pm 0.01	0.382 \pm 0.02	0.414 \pm 0.01	0.369 \pm 0.04	0.396 \pm 0.03
Electricity	96	0.197 \pm 0.01	0.312 \pm 0.01	0.190 \pm 0.00	0.306 \pm 0.00	0.188 \pm 0.00	0.303 \pm 0.00	0.188 \pm 0.00	0.303 \pm 0.01
	192	0.219 \pm 0.01	0.329 \pm 0.01	0.206 \pm 0.01	0.320 \pm 0.01	0.207 \pm 0.00	0.320 \pm 0.00	0.197 \pm 0.00	0.310 \pm 0.00
	336	0.263 \pm 0.04	0.359 \pm 0.03	0.236 \pm 0.02	0.344 \pm 0.01	0.237 \pm 0.03	0.344 \pm 0.02	0.224 \pm 0.02	0.333 \pm 0.01
	720	0.290 \pm 0.05	0.380 \pm 0.02	0.260 \pm 0.01	0.368 \pm 0.01	0.261 \pm 0.01	0.369 \pm 0.01	0.249 \pm 0.01	0.358 \pm 0.01
Traffic	96	0.628 \pm 0.02	0.393 \pm 0.02	0.605 \pm 0.01	0.380 \pm 0.01	0.594 \pm 0.02	0.367 \pm 0.01	0.567 \pm 0.00	0.350 \pm 0.00
	192	0.634 \pm 0.01	0.401 \pm 0.01	0.626 \pm 0.01	0.393 \pm 0.01	0.600 \pm 0.01	0.369 \pm 0.00	0.589 \pm 0.01	0.360 \pm 0.01
	336	0.619 \pm 0.01	0.385 \pm 0.01	0.635 \pm 0.01	0.400 \pm 0.00	0.625 \pm 0.01	0.386 \pm 0.01	0.619 \pm 0.01	0.383 \pm 0.01
	720	0.656 \pm 0.01	0.403 \pm 0.01	0.697 \pm 0.03	0.439 \pm 0.01	0.678 \pm 0.02	0.422 \pm 0.02	0.642 \pm 0.01	0.397 \pm 0.01

D Pseudocode of the Method

Algorithm 1 details the sequence of operations performed during the forward pass of the proposed model:

Algorithm 1 Scaleformer: Iterative Multi-scale Refining Transformer

Require: input lookback window $\mathbf{X}^{(L)} \in \mathbb{R}^{\ell_L \times d_x}$, scale factor s , a set of scales $S = \{s^m, \dots, s^2, s^1, 1\}$, Horizon length ℓ_H , and Transformer module F .

for $i \leftarrow 0$ to m **do**

- $\mathbf{X}_i^{\text{enc}} \leftarrow \text{AvgPool}(\mathbf{X}^{(L)}, \text{window_size} = s^{m-i})$ ▷ Equation (1) and (2) of the paper
- if** $i = 0$ **then**

 - $\mathbf{X}_i^{\text{dec}} \leftarrow \left[\vec{0}^{\ell_H} \right]$

- else**

 - $\mathbf{X}_i^{\text{dec}} \leftarrow \text{Upsample}(\mathbf{X}_{i-1}^{\text{out}}, \text{scale} = s)$ ▷ Equation (5) and (6) of the paper

- end if**
- $\bar{\mu}_{\mathbf{X}_i} \leftarrow \frac{1}{\ell_{L,i} + \ell_{H,i}} \left(\sum_{\mathbf{x}^{\text{enc}} \in \mathbf{X}_i^{\text{enc}}} \mathbf{x}^{\text{enc}} + \sum_{\mathbf{x}^{\text{dec}} \in \mathbf{X}_i^{\text{dec}}} \mathbf{x}^{\text{dec}} \right)$
- $\hat{\mathbf{X}}_i^{\text{dec}} \leftarrow \mathbf{X}_i^{\text{dec}} - \bar{\mu}_{\mathbf{X}_i}$
- $\hat{\mathbf{X}}_i^{\text{enc}} \leftarrow \mathbf{X}_i^{\text{enc}} - \bar{\mu}_{\mathbf{X}_i}$
- $\mathbf{X}_i^{\text{out}} \leftarrow F(\mathbf{X}_i^{\text{enc}}, \hat{\mathbf{X}}_i^{\text{dec}}) + \bar{\mu}_{\mathbf{X}_i}$

end for

Ensure: $\mathbf{X}_{\cdot}^{\text{out}}$ ▷ return the prediction at all scales

E Effect of α on the loss function

Figure 6 shows the impact of α on the shape of the loss function on the left, and example ground truth time-series corresponding to the horizon window on the right. As noted in the main paper, lower values of α tend to result in better robustness to outliers. This is indeed confirmed empirically in the case of the weather dataset, which corresponds to the lowest learnt α value, and has the outliers with the largest relative scales. For simplicity, we have excluded c on the analysis as it does not impact the robustness with regards to the outliers, as shown in [37].

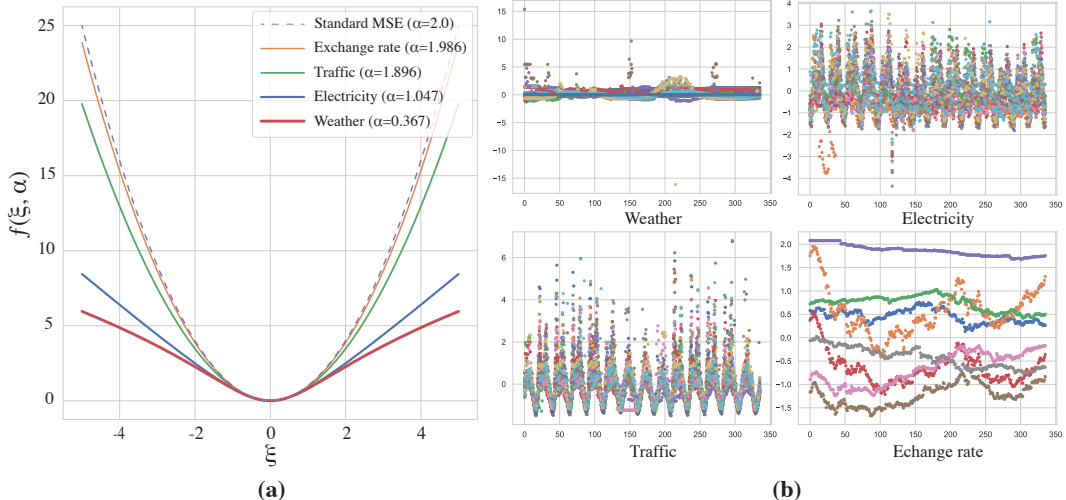


Figure 6: (a) The loss value based as a function of the ξ (absolute difference between prediction and target) and the learned α for each dataset. Different colors correspond to different datasets (each with specific value of α). (b) Samples taken from the ground-truth horizon window of each dataset. The Weather dataset sample has the outliers with the largest scales compared to the input series. As a consequence, the learnt value of α is the lowest. Different colors correspond to different variables in the multi-variate time-series we are considering.

F Additional qualitative results

Figure 7 provides additional qualitative results corresponding to the comparison between the baselines and our approach. As we can see, Scaleformer is able to better learn local and global time-series variations.

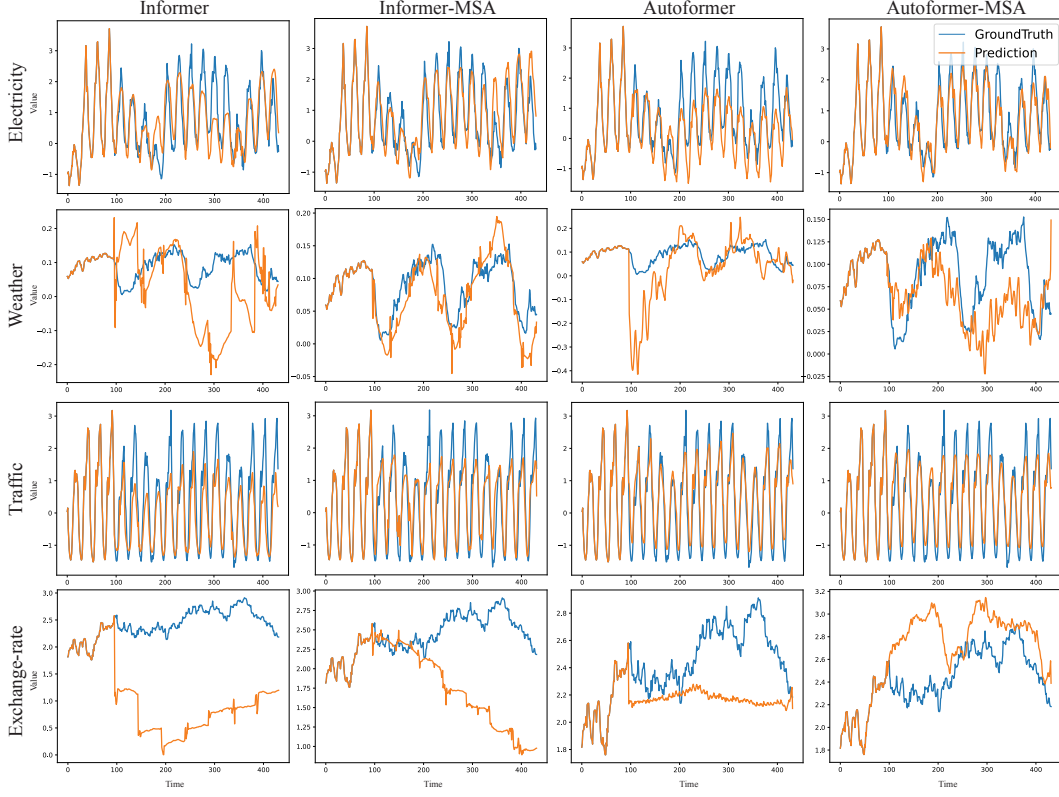


Figure 7: Additional qualitative comparison of the baselines against our framework.